

# 000 001 002 003 004 005 006 007 008 009 010 011 012 013 014 015 016 017 018 019 020 021 022 023 024 025 026 027 028 029 030 031 032 033 034 035 036 037 038 039 040 041 042 043 044 045 046 047 048 049 050 051 052 053 MULTIMODAL SOCIAL INTERACTION WITH MULTI-SPEAKER ATTENTION ALIGNMENT

Anonymous authors

Paper under double-blind review

## ABSTRACT

Understanding social interaction in video requires reasoning over a dynamic interplay of verbal and non-verbal cues: who is speaking, to whom, and with what gaze or gestures. While Multimodal Large Language Models (MLLMs) are natural candidates, simply adding visual inputs yields surprisingly inconsistent gains on social tasks. Our quantitative analysis of cross-modal attention inside state-of-the-art MLLMs reveals a core failure mode: in multi-speaker scenes, visual and textual tokens lack speaker-consistent alignment, exhibiting substantially weaker cross-modal attention than in object-centric images. To address this, we propose a multimodal multi-speaker attention alignment method that can be integrated into existing MLLMs. First, we introduce *dynamic cross-modal head selection* to identify attention heads most responsible for grounding. Then, an *adaptive social-aware attention bias*, computed from existing attention patterns and speaker locations, is injected into the attention mechanism. This bias reinforces alignment between a speaker’s visual representation and their utterances without introducing trainable parameters or architectural changes. Experiments on three datasets (TVQA+, MMSI, and OnlineMMSI) across four social tasks demonstrate that our approach improves the ability of MLLMs and achieves state-of-the-art results on multiple tasks. Attention visualizations confirm our method successfully focuses the model on speaker-relevant regions, enabling more robust multi-party social reasoning.

## 1 INTRODUCTION

Understanding social interaction requires modeling multi-party human behaviors through both verbal and non-verbal cues, including dialogue, gestures (Cao et al., 2025), gaze (Zhou et al., 2024), and facial expressions (Hyun et al., 2024). To study these interactions, prior works have proposed a variety of tasks and benchmarks, such as video question answering (VQA), speaking target detection, mentioned player prediction, and pronoun coreference resolution (Lei et al., 2020; Lee et al., 2024a). Beyond serving as evaluation platforms, these tasks underpin socially intelligent AI agents that operate in real-world multi-party scenarios like board games, daily conversations, and meetings.

Given their ability to comprehend both verbal and non-verbal information, multimodal large language models (MLLMs) are natural candidates for these tasks (Lee et al., 2024a; Li et al., 2025a; Park et al., 2025b). However, our analysis reveals a critical limitation: the addition of visual information does not consistently improve, and can even degrade their performance in multi-person settings. For example, on OnlineMMSI (Li et al., 2025a), supplying video frames to Qwen2.5-VL (Bai et al., 2025) input yields no gain on the mentioned player prediction task, while LLaMA-3.2-Vision (Dubey et al., 2024) sees its performance drop on the pronoun coreference resolution task (Li et al., 2025a). These observations suggest that current MLLMs struggle to effectively exploit multimodal cues in complex multi-person social settings.

To better understand why MLLMs fail to leverage multimodal cues, we conduct a systematic quantitative analysis of cross-modal attention weights inside state-of-the-art MLLMs (Bai et al., 2025). By measuring the attention weights between a speaker’s textual tokens and their corresponding visual region (i.e., their bounding box), we uncover a stark deficiency. We find that the cross-modal alignment in multi-person videos is significantly weaker and less focused compared to the alignment observed in general object-centric datasets like COCO (Lin et al., 2014). This limitation results in

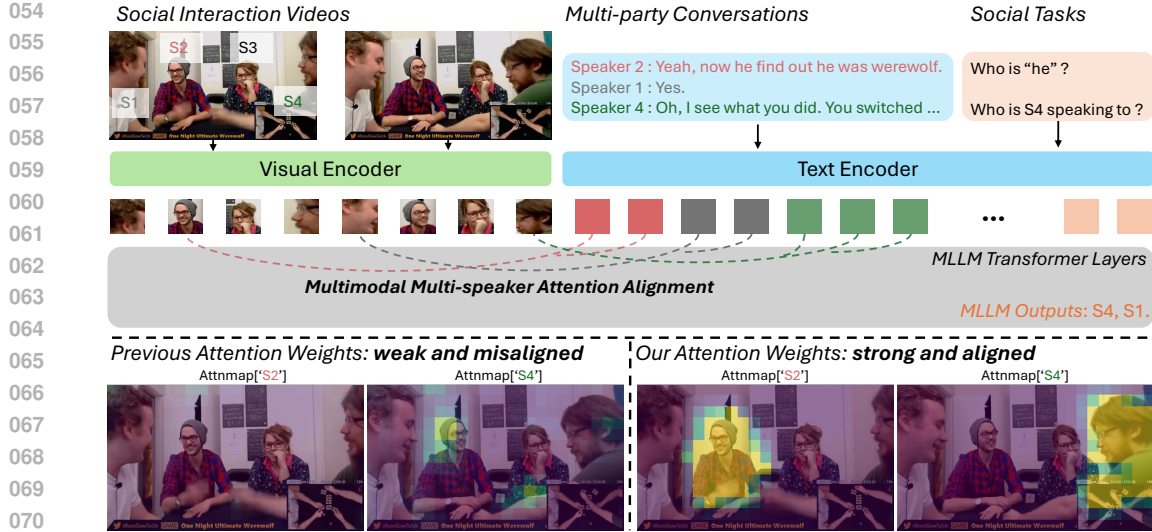


Figure 1: We propose a multimodal multi-speaker attention alignment method for MLLMs to understand social interactions in videos. Visualization of cross-attention weights in transformer layers confirms that our approach strengthens the model’s focus on areas relevant to the active speaker.

inconsistent alignment between visual and textual modalities, thereby constraining the effectiveness of MLLMs in multi-person social tasks.

To address this misalignment problem, we propose a multimodal multi-speaker attention alignment method. Our approach intervenes directly within the transformer’s cross-attention layers. We first propose a **dynamic cross-modal head selection** strategy that identifies attention heads most responsible for visual-text grounding. We then apply an **adaptive social-aware attention bias** to these heads, which amplifies the attention scores between the visual and textual tokens belonging to the same speaker. As illustrated in fig. 1, this mechanism explicitly guides the model to associate the correct visual features with the corresponding dialogue. Crucially, our method requires no additional trainable parameters or architectural changes in models.

We evaluate our method on three multimodal social interaction benchmarks (TVQA+ (Lei et al., 2020), MMSI (Lee et al., 2024a), and OnlineMMSI (Li et al., 2025a)) across four representative tasks. Integrated into Qwen2.5-VL (Bai et al., 2025), our method consistently outperforms strong baselines, yielding an average accuracy improvement of 3.5%. It achieves state-of-the-art performance on three task settings and remains highly competitive on the remaining one. Attention visualizations further confirm that our approach successfully guides the model to focus on speaker-relevant regions in videos.

Our main contributions are summarized as follows:

- We are the first to systematically quantify and identify the cross-modal attention misalignment in MLLMs as a key bottleneck for understanding multi-party social interactions.
- We propose a novel attention alignment method that dynamically reinforces the association between speakers’ visual and textual representations without additional trainable parameters.
- Extensive experiments demonstrate that our method effectively guides model attention to speaker-relevant regions, thereby improving performance in diverse multimodal social interaction tasks.

## 2 RELATED WORKS

### 2.1 MULTIMODAL SOCIAL INTERACTION

Multimodal social interaction refers to human communication across multiple modalities, including spoken language, facial expressions (Hyun et al., 2024), gaze (Zhou et al., 2024), gestures (Cao et al., 2025), and body movements (Balazia et al., 2022). Prior research has proposed a variety of

related tasks and benchmarks, such as video question answering (VQA) (Lei et al., 2018; Zadeh et al., 2019; Hyun et al., 2024; Mathur et al., 2025; Kong et al., 2025), conversational modeling (Ryan et al., 2023; Lee et al., 2024a; Jia et al., 2024; Chang et al., 2025), speaker prediction (Northcutt et al., 2020; Müller et al., 2021), and social behavior classification (Lai et al., 2023; Cao et al., 2025). These tasks hold strong potential for enabling AI agents to operate in multi-party social scenarios, including board games (Lai et al., 2023; Grauman et al., 2022), daily conversations (Northcutt et al., 2020), and multi-person meetings (Müller et al., 2018; Kraaij et al., 2005). Leveraging MLLMs for such social interaction tasks has recently become an emerging trend (Lee et al., 2024b; Mathur et al., 2024; Mou et al., 2024). This work is the first to introduce a multimodal attention alignment method for multi-person conversations, evaluated across three datasets and four social interaction tasks, showing its capacity to generalize across diverse multimodal social interaction tasks and benchmarks.

## 2.2 MULTIMODAL BIAS AND ALIGNMENT IN MLLMs

In multimodal learning, diverse modalities have been incorporated into MLLMs (Liu et al., 2023; Yan et al., 2024), where one fundamental challenge is achieving effective cross-modal alignment (Radford et al., 2021; Girdhar et al., 2023; Chen et al., 2024c; Amirloo et al., 2024; Li et al., 2025b). Recent studies (Wu et al., 2024b; Amirloo et al., 2024; Xiao et al., 2024; Zheng et al., 2025; Park et al., 2025b; Zhang et al., 2025d) have highlighted that MLLMs are deeply affected by modality bias, where the models’ understanding and reasoning capabilities rely heavily on the textual modality while underutilizing other modalities. To mitigate this bias and align modalities, some approaches have focused on collecting additional datasets (Chen et al., 2024a; Wu et al., 2024c; Yue et al., 2024; Chen et al., 2024b), reinforcement learning (Pi et al., 2024; Sun et al., 2024; Zhang et al., 2025b;c), while other methods have sought to adjust the model’s attention toward non-text modalities (Xing et al., 2024; Zhang et al., 2024; Tong et al., 2024; Song et al., 2025; An et al., 2025; Tang et al., 2025; Wang et al., 2025; Zhang et al., 2025a). These methods have demonstrated effectiveness on tasks such as VQA, but they lack evaluation and exploration in multi-speaker social interaction scenarios.

Existing work on multimodal social interaction has proposed several strategies for aligning visual and textual modalities across multiple speakers. (Lee et al., 2024a) uses speaker embeddings (Devlin et al., 2019), (Li et al., 2025a) leverages visual prompts (Shtedritski et al., 2023), (Park et al., 2025a) introduces Chain-of-Thought, and (Agrawal et al., 2024) incorporates the audio modality for alignment. Compared to these works on social interactions, our study is the first to systematically and quantitatively investigate this misalignment in social benchmarks. We are also the first to utilize the cross-attention map within transformer layers for multi-person social interaction tasks.

## 3 ANALYSIS OF CROSS-MODAL ALIGNMENT IN MULTI-SPEAKER SETTINGS

Alignment between modalities is a fundamental challenge in vision-language models (VLMs) and multimodal large language models (MLLMs), and a large body of work has focused on learning aligned representations between visual and textual encoders (Radford et al., 2021). This alignment can be quantitatively assessed via the cross-modal attention weights between textual and visual features (Alayrac et al., 2022). When the visual tokens  $\mathcal{V}$  and textual tokens  $\mathcal{U}$  are concatenated and processed by a transformer, the self-attention mechanism (Vaswani et al., 2017) enables interactions across modalities. Formally, let  $\mathcal{X} = [\mathcal{V}; \mathcal{U}] \in \mathbb{R}^{(THW+K) \times d}$  denote the concatenated token sequence. The attention weights are computed as

$$\text{Attn}(i, j) = \text{softmax}_j \left( \frac{(x_i W_Q)(x_j W_K)^\top}{\sqrt{d}} \right), \quad (1)$$

where  $x_i, x_j \in \mathcal{X}$  are token embeddings and  $W_Q, W_K$  are projection matrices. In the cross-modal case, we specifically focus on the sub-matrix of  $\text{Attn}(i, j)$  where  $i$  indexes text tokens and  $j$  indexes visual tokens. This sub-matrix, denoted as the **cross-modal attention weights**, captures the semantic grounding between textual and visual modalities. High attention weights in this matrix indicate that tokens from text effectively attend to semantically corresponding visual tokens. For example, as illustrated in fig. 2 (a), tokens representing “cat”, “car”, and “flower” attend strongly to visual tokens corresponding to object regions. Such interpretable cross-modal attention maps have been widely utilized in multimodal tasks, including MLLMs for visual grounding (Wu et al., 2024a; Zhang et al., 2025a) and text-to-image generation models (Chefer et al., 2023; Hertz et al., 2023).

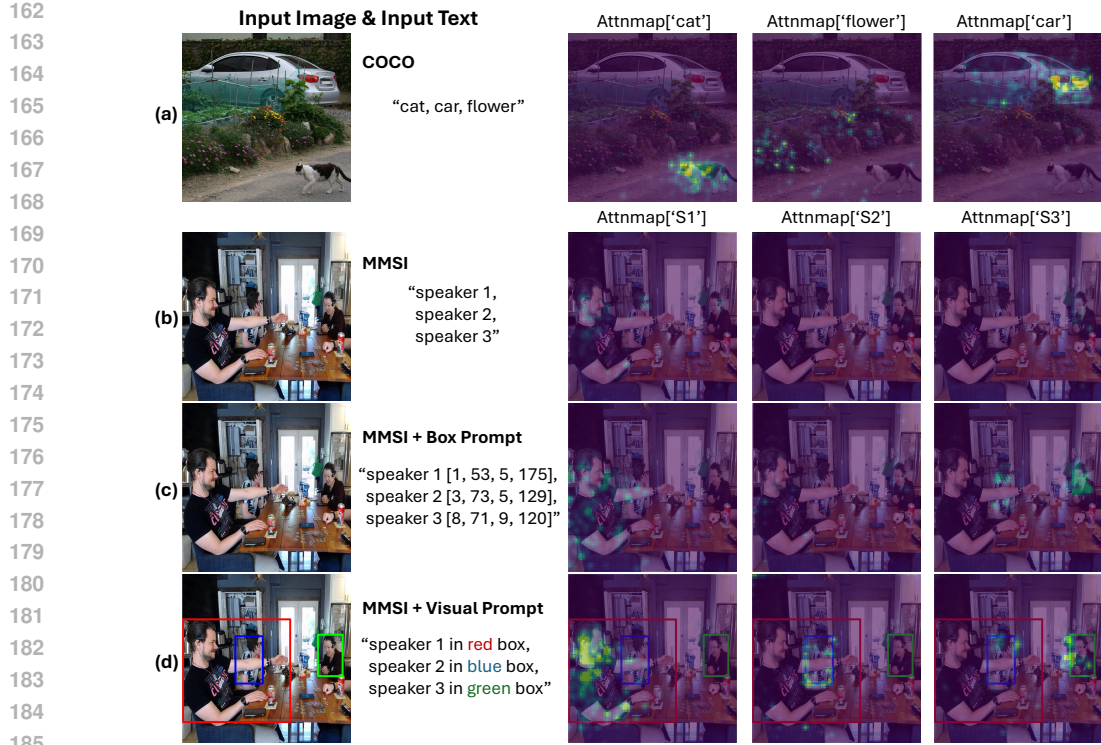


Figure 2: Cross attention weights in Qwen2.5-VL layer 16. Compared to general images, cross-modal alignment in multi-speaker images is weak and inconsistent. Image resolution is 2000x2000.

In multi-speaker social interaction scenarios, challenges arise due to the presence of multiple individuals in the visual scene and ambiguous textual references in conversations. For example, speakers are often mentioned by names or anonymized labels such as “speaker 2”, which do not clearly correspond to visual regions. As illustrated in fig. 2 (b), the attention weights of speakers’ textual tokens are highly scattered, preventing the model from effectively leveraging the corresponding visual information. One attempt to mitigate this issue is shown in fig. 2 (c), where bounding box coordinates are prompted into the text input. However, we observe that the resulting cross-modal attention remains weak, and the model still struggles to establish clear correspondences. Previous works (Li et al., 2025a; Shtedritski et al., 2023) have also proposed introducing visual prompts, such as adding highlighted bounding boxes or keypoints in the image (fig. 2 (d)). This strategy indeed helps speakers’ textual tokens attend to the correct region, but the attention tends to concentrate along the bounding box boundaries rather than the interior. Moreover, we find that the attention map of speaker 3 becomes misaligned, incorrectly overlapping with the region of speaker 2.

To investigate how well MLLMs align textual references with visual evidence in multi-speaker images, we quantitatively analyze cross-modal attention through controlled experiments with Qwen2.5-VL (Bai et al., 2025). Specifically, given a text token  $u_i \in \mathcal{U}$  and its corresponding visual tokens  $\mathcal{V}_s \subset \mathcal{V}$ , we define the alignment score as

$$AttnMax(u_i, \mathcal{V}_s) = \max_{v \in \mathcal{V}_s} Attn(u_i, v), \quad AttnMean(u_i, \mathcal{V}_s) = \frac{1}{|\mathcal{V}_s|} \sum_{v \in \mathcal{V}_s} Attn(u_i, v) \quad (2)$$

We compute such statistics across different datasets and compare under various alignment strategies.

**COCO** (Lin et al., 2014). We sample 1,110 images from the COCO object detection validation set, and compute attention with text queries such as “{class 1}, {class 2}, …”.

**MMSI** (Lee et al., 2024a). We use 1,921 images with queries “{speaker 1}, {speaker 2}, …”.

**MMSI + Box Prompt** (Bai et al., 2025). The text input is augmented with bounding box coordinates, e.g., “{speaker 1} in [x,y,z,t], {speaker 2} in [a,b,c,d], …”.

**MMSI + Visual Prompt** (Li et al., 2025a). Bounding boxes are drawn in distinct colors on the image, and the query takes the form “{speaker 1} in red box, {speaker 2} in blue box, …”.

216 **Ours.** We apply our proposed multi-speaker alignment method, which explicitly enhances attention  
 217 weights in speaker-specific regions. See section 4 for details.  
 218

219 Table 1: Cross attention weights in COCO and MMSI images.

220 <b>Image Source</b>	221 <b>Alignment Method</b>	222 <i>AttnMax</i> $\times 10^{-2}$	223 <i>AttnMean</i> $\times 10^{-4}$
222 COCO	/	9.23	15.56
		4.54	3.26
	box prompt	4.49	3.93
	visual prompt	6.29	5.29
224 MMSI	Ours	<b>17.09</b>	<b>26.20</b>

227 We report the quantitative results in table 1. Compared to general objects in COCO detection dataset,  
 228 the attention between images and speaker tokens in MMSI is substantially lower, highlighting the  
 229 difficulty of aligning speaker references in multi-person contexts. We further observe that introducing  
 230 visual prompts indeed improves attention weights, but the gains remain limited. This reveals a  
 231 fundamental challenge for MLLMs: cross-modal alignment for multi-speaker scenarios is weak and  
 232 inconsistent, as the model struggles to establish clear correspondences between textual references to  
 233 speakers and their visual representations.  
 234

235 

## 4 PROPOSED METHOD

236 To address the problem of weak and inconsistent cross-modal alignment in social tasks, we propose  
 237 a multimodal multi-speaker attention alignment method. Our approach consists of two key com-  
 238 ponents: (1) a dynamic cross-modal head selection mechanism that identifies attention heads most  
 239 relevant for multimodal grounding, and (2) an adaptive social-aware attention bias that reinforces  
 240 cross-modal token alignment. An overview of the method is illustrated in fig. 3.  
 241

242 **Input for MLLMs.** Let the social interaction video be mapped into a set of visual tokens  $\mathcal{V} =$   
 243  $\{v_{t,h,w} \in \mathbb{R}^d \mid t \in [1, T], h \in [1, H], w \in [1, W]\}$  by the patch embedder and visual encoder, where  
 244 each token corresponds to a spatio-temporal patch indexed by  $(t, h, w)$ . The transcripts consist  
 245 of speakers’ utterances, which are tokenized and encoded into  $\mathcal{U} = \{u_k \in \mathbb{R}^d \mid k \in [1, K]\}$ ,  
 246 where each token  $u_k$  is associated with a speaker label  $s$  and a timestamp  $t$ . In general, the speaker  
 247 label  $s$  is determined by who speaks the utterance, except for certain special tokens that explicitly  
 248 refer to speakers (e.g., “Mitchell” or “speaker 2”), which are consistently assigned the label of the  
 249 person they denote. Note that textual contents unrelated to speaker utterances, such as the system  
 250 prompt and task instructions, are not included in  $\mathcal{U}$ . In addition, the dataset provides a set of speaker  
 251 bounding boxes  $\mathcal{B} = \{b_{s,t}\}$ , where each box  $b_{s,t}$  specifies the spatial location of speaker  $s$  at frame  
 252  $t$ . By mapping box coordinates to the grid of visual tokens, we obtain subset  $\mathcal{V}_{s,t}$  associated with  
 253 each speaker label.  
 254

255 

### 4.1 DYNAMIC CROSS-MODAL HEAD SELECTION

256 Modern MLLMs employ multi-head attention, with different heads capturing complementary facets  
 257 of token interactions (Vaswani et al., 2017; Voita et al., 2019). Previous studies (Bi et al., 2025)  
 258 in MLLMs have identified that specific transformer layers contain specialized “visual heads” that  
 259 reliably focus on image tokens during task-solving. The presence and focus of such heads vary  
 260 across models and training strategies, indicating that visual heads are dynamic rather than fixed.  
 261

262 To preserve the pretrained capabilities of MLLMs while improving their cross-modal grounding, we  
 263 propose a dynamic cross-modal head selection mechanism that identifies the subset of heads with  
 264 strong cross-modal interactions. Concretely, let  $\mathcal{V}_{all} = \bigcup_{s \in S} \bigcup_{t \in T} \mathcal{V}_{s,t}$  denote the set of visual  
 265 tokens inside bounding boxes for all speakers in the video. We define a threshold  $\lambda$  to classify  
 266 each attention head, based on the cross-modal attention sub-matrix  $\text{Attn}(\mathcal{U}, \mathcal{V}_{all})$  that represents the  
 267 attention from utterance tokens to all speaker regions:  
 268

$$269 \text{head is } \begin{cases} \text{active,} & \frac{1}{|\mathcal{U}| |\mathcal{V}_{all}|} \sum_{u \in \mathcal{U}} \sum_{v \in \mathcal{V}_{all}} \text{Attn}_{head}(u, v) > \lambda, \\ \text{inactive,} & \text{otherwise.} \end{cases} \quad (3)$$

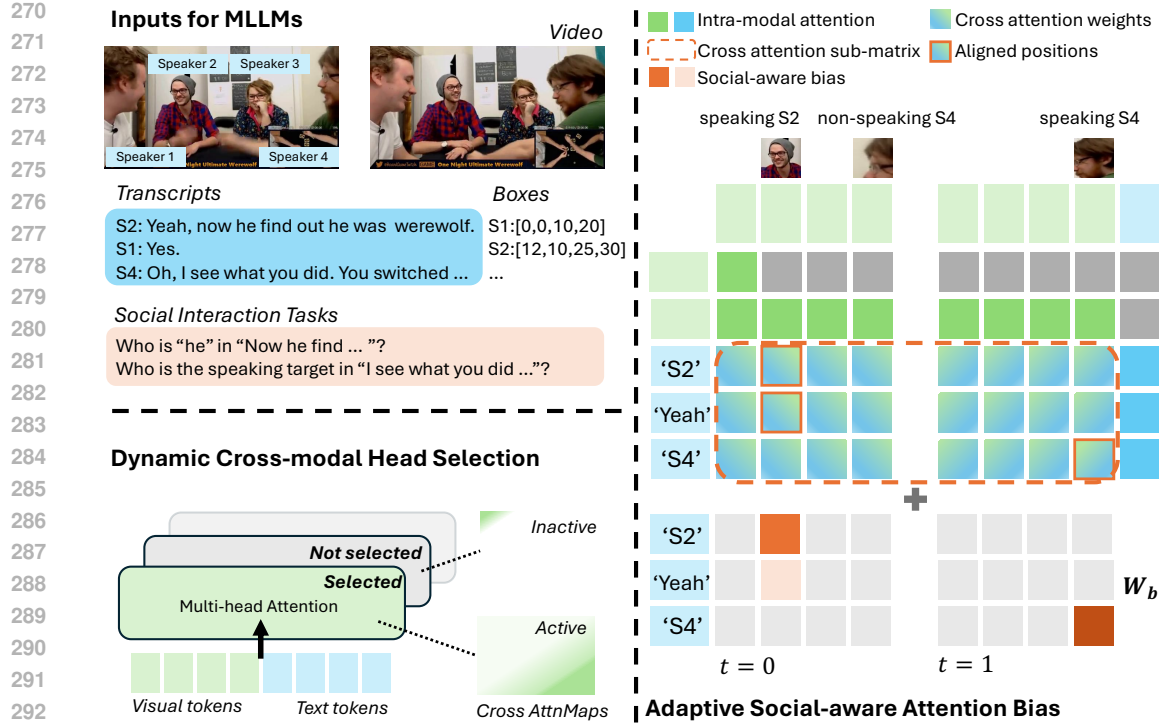


Figure 3: Overview of proposed method.

As illustrated in fig. 3, an *active* head is characterized by having distinctly high attention weights concentrated in one or more speaker regions, whereas an *inactive* head exhibits weak cross-modal attention across all regions. Only active heads are selected for applying the subsequent social-aware attention bias.

#### 4.2 ADAPTIVE SOCIAL-AWARE ATTENTION BIAS

In attention computation, adding a bias term to attention weights is a common strategy to control token interactions. For example, language models introduce padding masks or causal masks to prevent tokens from attending to irrelevant or future positions (Devlin et al., 2019; Radford et al., 2019). In the context of social interaction, to strengthen the attention between visual and textual tokens belonging to the same speaker  $s$  in frame  $t$ , we introduce a *social-aware bias*  $W_b$  applied within the active heads. Specifically, for a text token  $u_i$  associated with speaker  $s$ , we assign the bias value for each visual token  $v_j$  as

$$W_b(u_i, v_j) = \alpha \cdot \max_{v \in \mathcal{V}_{all}} \frac{(u_i W_Q)(v W_K)^\top}{\sqrt{d}}, \quad u_i \in \mathcal{U}_{s,t}, \quad v_j \in \mathcal{V}_{s,t}, \quad (4)$$

where  $\alpha$  is a scaling factor controlling the bias strength, and  $\max_{v \in \mathcal{V}_{all}} \text{Attn}(u_i, v)$  captures the strongest cross-modal interaction that  $u_i$  originally attends to among all speakers' visual tokens.

The motivation of using adaptive weights for different tokens is that certain tokens (e.g., "speaker", "Sheldon", or object mentions) naturally exhibit stronger semantic interactions with visual content, while others (e.g., discourse fillers such as "yeah", "then") are much weaker. By assigning the maximum attention value to speaker-associated regions, we softly shift the distribution of attention towards the visual area of the current speaker, without suppressing the token's original attention pattern. This design ensures that attention alignment is enhanced in a smooth and adaptive way rather than enforced rigidly. Finally, the adjusted attention is computed as:

$$\widetilde{\text{Attn}}(i, j) = \text{softmax}_j \left( \frac{(u_i W_Q)(v_j W_K)^\top}{\sqrt{d}} + W_b(u_i, v_j) \right). \quad (5)$$

Our method requires no additional trainable parameters. Moreover, by leveraging dynamic head selection, it introduces only minimal computational overhead while effectively utilizing speaker bounding box annotations to enhance cross-modal alignment in multi-speaker videos.

324 

## 5 EXPERIMENTS

325 

### 5.1 DATASETS

328 We conduct experiments on three publicly available datasets under four social task settings. These  
 329 datasets contain videos, timestamped transcripts, and speaker bounding box annotations, which are  
 330 utilized in both training and evaluation. The datasets statistics are described below:

331 **TVQA+** (Lei et al., 2020; 2018) is a multi-party video question answering dataset with rich dynamics-  
 332 and realistic social interactions built on TV series. The QA-pairs are diverse, covering dialogue  
 333 understanding, reasoning, and speaker relations modeling. In our experiments, we select samples  
 334 containing at least one annotated speaker bounding box, resulting in 17,306 training samples and  
 335 2,211 test samples. On average, each sample involves 1.9 speakers, 23.8 words and 7.8 seconds.

336 **MMSI** (Lee et al., 2024a) is a recent social interaction benchmark built from multi-party board  
 337 game videos (Lai et al., 2023) collected from YouTube and Ego4D (Grauman et al., 2022). It defines  
 338 three challenging tasks to capture fine-grained interaction dynamics: speaking target identification,  
 339 pronoun coreference resolution, and mentioned player prediction. Following their split and prepro-  
 340 cessing, we use the YouTube subset, which contains 7,111 training samples and 1,921 test samples.  
 341 On average, each sample involves 4.1 speakers, 85.2 words, and 3.0 seconds of video.

342 **OnlineMMSI** (Li et al., 2025a) is an extension of MMSI that reformulates three tasks under an  
 343 online setting, where only preceding context of a conversation is available, without access to future  
 344 dialogue. This design increases task difficulty and enhances practical applicability. The data split  
 345 and statistics is identical to MMSI, with a forward-shifted historical window applied to each sample.

347 

### 5.2 IMPLEMENTATION DETAILS

349 We adopt Qwen2.5-VL-Instruct-7B (Bai et al., 2025) as the base MLLM in all experiments. Fol-  
 350 lowing dataset annotations (Lei et al., 2020; Lee et al., 2024a), videos are processed at resolution of  
 351 640×360 and uniformly sampled into 8 frames. During training, we fine-tune the model using LoRA  
 352 (Hu et al., 2022) applied to all projection layers. Following (Li et al., 2025a), we set the LoRA rank  
 353 to 512, the learning rate to 1e-4, the batch size to 4, and train for 5 epochs. All experiments are con-  
 354 ducted on a single NVIDIA A100 GPU, with the implementation built on LLaMA-Factory (Zheng  
 355 et al., 2024) and pytorch (Paszke et al., 2019). We set  $\lambda = 5e-5$  and  $\alpha = 1.0$  in our method. The  
 356 prompts used for MLLM instructions are provided in appendix A.1.

357 

### 5.3 RESULTS

359 Table 2: Accuracy on TVQA+, MMSI and OnlineMMSI.  $T$  for speaking target identification,  $P$   
 360 for pronoun coreference resolution,  $M$  for mentioned speaker prediction. \* TLNet/ST-VLM results  
 361 are taken from their paper, which may adopt a different split from ours. More descriptions of the  
 362 baselines are provided in appendix A.2.

364 <b>Method</b>	365 <b>TVQA+ VideoQA</b>	366 <b>MMSI</b>			367 <b>OnlineMMSI</b>		
		368 <i>T</i>	369 <i>P</i>	370 <i>M</i>	371 <i>T</i>	372 <i>P</i>	373 <i>M</i>
374 Random	375 20.0	376 21.0	377 23.2	378 23.7	379 21.0	380 23.2	381 23.7
382 ST-VLM-7B* (Ko et al., 2025)	383 68.1						
384 TLNet* (Liang et al., 2024a)	385 75.5						
386 MMSI (Lee et al., 2024a)	387 74.5	388 73.0	389 62.5	390 59.1	391 63.4	392 47.3	
393 OnlineMMSI (Li et al., 2025a)	394 86.1	395 66.5	396 76.2	397 63.5	398 64.8	399 72.9	400 49.4
391 Qwen2.5-Text (Bai et al., 2025)	392 78.0	393 66.3	394 77.0	395 61.7	396 59.3	397 74.4	398 49.0
399 Qwen2.5-VL (Bai et al., 2025)	400 85.1	401 63.3	402 77.2	403 58.3	404 59.6	405 75.1	406 50.2
407 <b>Qwen2.5-VL+Ours</b>	408 <b>87.3</b>	409 <b>68.5</b>	410 <b>78.6</b>	411 <b>66.0</b>	412 <b>62.4</b>	413 <b>78.2</b>	414 <b>53.1</b>

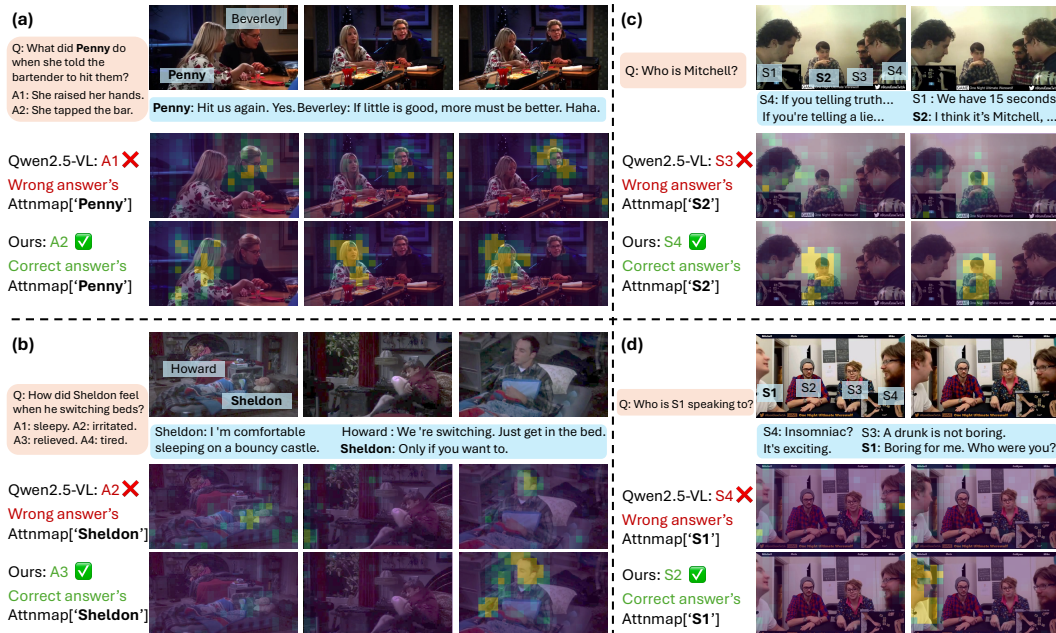
375 **Comparison with baselines** table 2 presents the accuracy on TVQA+, MMSI, and OnlineMMSI.  
 376 On TVQA+, our method improves Video Multiple-Choice QA accuracy by 2.1% over Qwen2.5-  
 377 VL, achieving a new state-of-the-art result. On MMSI and OnlineMMSI, our approach yields gains  
 378 of 4.0%, 2.5%, and 5.3% across three social tasks, demonstrating that our method significantly

378 enhances MLLMs’ ability to understand social interaction. We observe that the improvements on  
 379 MMSI are higher than on TVQA+. This is because MMSI videos involve more participants, high-  
 380 lighting the advantage of our approach in handling multi-speaker alignment under more complex  
 381 scenarios. In addition, TVQA+ videos are drawn from scripted TV shows, where speaker char-  
 382 acters are fixed and the model may learn name-token associations during finetuning. Compared to  
 383 baselines that rely on injecting box coordinates, speaker names, or color cues into the text input  
 384 to associate modalities, our method requires no such auxiliary prompts. While their improvements  
 385 are often unstable across tasks (boosting performance on some tasks while degrading others), our  
 386 method modifies attention distributions in a natural and direct manner, achieving stable and gener-  
 387 alizable cross-modal alignment for social interaction tasks.

388 On the other hand, our method does not surpass the current state-of-the-art on the speaking target  
 389 identification task, likely because this task requires more balancing attention between both the cur-  
 390 rent speaker and the his speaking target. However, we still achieves the second-best accuracy with  
 391 competitive performance, and on pronoun coreference resolution and mentioned speaker prediction,  
 392 our approach significantly outperforms prior methods on MMSI and OnlineMMSI.

393 **Visualizations** We present visualizations of Qwen2.5-VL’s cross-attention maps before and after  
 394 applying our social-aware bias in fig. 4. As shown in example (a), when asked about the behavior of  
 395 the character Penny, Qwen2.5-VL incorrectly predicted “raise hand”, which is actually the action of  
 396 another character, Beverley. The attention map reveals that a considerable portion of Penny’s atten-  
 397 tion was misaligned to Beverley’s region. After adding our bias, the attention naturally concentrates  
 398 on Penny, leading to the correct answer “tap the bar”.

399 In the case (b), the question concerns the emotion of Sheldon when switching beds (third image, cor-  
 400 responding to Sheldon’s second utterance). We visualize the attention maps of the second “Sheldon”  
 401 token across frames. Without our bias, Qwen2.5-VL assigns attention uniformly across Sheldon’s  
 402 visual tokens over all frames. By adding our bias, the model clearly emphasizes the third frame over  
 403 the first, achieving more accurate spatial–temporal–speaker alignment between text and video, and  
 404 producing the correct answer. Similarly, in two examples (c)(d) from MMSI, our bias enables precise  
 405 modeling of current speaker in videos, further enhancing the understanding of social interactions.



429 Figure 4: Attention maps in Qwen2.5-VL layer 16 before and after adding social-aware bias. Our  
 430 bias enables more accurate spatial–temporal–speaker alignment. Video resolution is 640x360.

432 5.4 ABLATIONS  
433434 To examine the effectiveness of different components of our method, we conduct ablations on active  
435 head selection and social-aware bias.436 **Transformer Layers** We investigate the effect of applying bias at different layers of the transformer,  
437 including all layers (0–27), as well as subsets of early, middle, and late layers. As shown in table 3,  
438 the best performance is achieved when the bias is applied to middle layers (10–19), followed by all  
439 layers. This finding suggests that middle layers may play a more crucial role in cross-modal feature  
440 fusion. This observation is consistent with prior studies (Zhang et al., 2025a; Liang et al., 2024b;  
441 Chen et al., 2025; Bi et al., 2025), as well as with our visualization analysis conducted on layer 16.442 **Active Head Threshold** We vary the cross-attention strength threshold  $\lambda$  and report the results with  
443 the ratio of active heads in table 4. Note that we only apply the bias to middle layers, thus the  
444 maximum ratio is 35.7%. We find that the best performance is achieved at a small threshold of  
445  $5e - 5$ . Compared to the original Qwen2.5-VL, even activating only 9% of heads yields an average  
446 improvement of about 3% across tasks, while activating 25% achieves a 4% gain. This demonstrates  
447 the importance of our bias in facilitating multi-speaker multimodal understanding. In contrast,  
448 activating all heads leads to a drop in performance, likely because some heads are responsible for  
449 attending positional encoding or text modality, while adding bias on them disrupts their stability.

450 451 Table 3: Effect of transformer layers.

Layers	TVQA+ VideoQA	MMSI		
		T	P	M
0-27	85.6	66.9	<b>79.1</b>	63.2
0-9	86.0	66.9	76.7	64.4
10-19	<b>87.3</b>	<b>68.5</b>	<u>78.6</u>	<b>66.0</b>
20-27	86.2	66.4	78.4	64.4

452 Table 4: Effect of the number of active heads.

$\lambda$	Active heads(%)	TVQA+ VideoQA	MMSI		
			T	P	M
0	35.7	85.6	65.4	77.8	61.2
5e-5	24.6	<b>87.3</b>	<b>68.5</b>	<u>78.6</u>	<b>66.0</b>
2e-4	15.8	86.8	67.9	78.2	66.0
8e-4	9.0	86.5	68.3	<b>78.8</b>	64.9
inf	0.0	85.1	63.3	77.2	58.3

460 **Bias Strength** We evaluate different strategies for setting  
461 the bias strength, with results shown in table 5. Compared to the fixed-value strategy, our adaptive  $W_b$   
462 in eq. (4) consistently achieves better performance. A  
463 fixed large bias forces the model to over-focus on the  
464 guided regions while ignoring global visual information,  
465 which in turn leads to a performance drop. This  
466 indicates that our adaptive social-aware biasing mecha-  
467 nism is highly natural: it enhances attention toward the  
468 current speaker’s region without disrupting the model’s  
469 inherent attention patterns, thereby improving cross-  
470 modal alignment and yielding stronger performance  
471 across social interaction tasks.473 6 CONCLUSION  
474475 This paper presents a method to help multimodal large language models better understand multi-  
476 modal multi-speaker social interactions. Building on a systematic analysis of cross-modal attention,  
477 the proposed method strengthens the alignment between visual and textual tokens belonging to the  
478 same speaker. Experiments across multiple datasets and tasks validate its effectiveness in improving  
479 multi-speaker reasoning. Future research directions include further investigating the role of attention  
480 heads in cross-modal alignment, exploring ways to leverage inherent grounding abilities of MLLMs  
481 to guide alignment without relying on bounding box annotations, thereby reducing annotation costs  
482 and enhancing efficiency for social AI.483 **LLM Usage** In this work, a large language model (ChatGPT) was employed solely for language  
484 polishing and writing refinement. Its role was limited to improving clarity and readability of the  
485 manuscript. LLM was **not** involved in the design of the methodology, data processing, or analysis.

486 Table 5: Effect of bias strength.

Bias	TVQA+ VideoQA	MMSI		
		T	P	M
fixed				
0	85.1	63.3	77.2	58.3
10	86.4	65.7	75.3	63.5
100	84.4	64.2	72.5	53.8
adaptive				
0.5 · max	86.8	66.8	77.2	63.7
1 · max	<b>87.3</b>	<b>68.5</b>	<u>78.6</u>	<b>66.0</b>
2 · max	86.0	66.7	77.4	64.1

486 REFERENCES  
487

488 Aviral Agrawal, Carlos Mateo Samudio Lezcano, Iqui Balam Heredia-Marin, and Prabhdeep Singh  
489 Sethi. Listen then see: Video alignment with speaker attention. In *Proceedings of the IEEE/CVF*  
490 *Conference on Computer Vision and Pattern Recognition Workshops*, pp. 2018–2027, June 2024.

491 Jean-Baptiste Alayrac, Jeff Donahue, Pauline Luc, Antoine Miech, Iain Barr, Yana Hasson, Karel  
492 Lenc, Arthur Mensch, Katherine Millican, Malcolm Reynolds, et al. Flamingo: a visual language  
493 model for few-shot learning. *Advances in neural information processing systems*, 35:23716–  
494 23736, 2022.

495 Elmira Amirloo, Jean-Philippe Fauconnier, Christoph Roesmann, Christian Kerl, Rinu Boney, Yusu  
496 Qian, Zirui Wang, Afshin Dehghan, Yinfei Yang, Zhe Gan, et al. Understanding alignment in  
497 multimodal llms: A comprehensive study. *arXiv preprint arXiv:2407.02477*, 2024.

498 Wenbin An, Feng Tian, Sicong Leng, Jiahao Nie, Haonan Lin, Qianying Wang, Ping Chen, Xiaoqin  
499 Zhang, and Shijian Lu. Mitigating object hallucinations in large vision-language models with  
500 assembly of global and local attention. In *Proceedings of the IEEE/CVF Conference on Computer*  
501 *Vision and Pattern Recognition*, pp. 29915–29926, June 2025.

502 Shuai Bai, Keqin Chen, Xuejing Liu, Jialin Wang, Wenbin Ge, Sibo Song, Kai Dang, Peng Wang,  
503 Shijie Wang, Jun Tang, et al. Qwen2. 5-vl technical report. *arXiv preprint arXiv:2502.13923*,  
504 2025.

505 Michal Balazia, Philipp Müller, Ákos Levente Tánczos, August von Liechtenstein, and François  
506 Brémond. Bodily behaviors in social interaction: Novel annotations and state-of-the-art eval-  
507 uation. In *Proceedings of the 30th ACM International Conference on Multimedia*, pp. 70–79,  
508 2022.

509 Jing Bi, Junjia Guo, Yunlong Tang, Lianggong Bruce Wen, Zhang Liu, Bingjie Wang, and Chenliang  
510 Xu. Unveiling visual perception in language models: An attention head analysis approach. In  
511 *Proceedings of the IEEE/CVF Conference on Computer Vision and Pattern Recognition (CVPR)*,  
512 pp. 4135–4144, June 2025.

513 Xu Cao, Pranav Virupaksha, Wenqi Jia, Bolin Lai, Fiona Ryan, Sangmin Lee, and James M Rehg.  
514 Socialgesture: Delving into multi-person gesture understanding. In *Proceedings of the IEEE/CVF*  
515 *Conference on Computer Vision and Pattern Recognition*, pp. 19509–19519, 2025.

516 Kent K Chang, Mackenzie Hanh Cramer, Anna Ho, Ti Ti Nguyen, Yilin Yuan, and David Bamman.  
517 Multimodal conversation structure understanding. *arXiv preprint arXiv:2505.17536*, 2025.

518 Hila Chefer, Yuval Alaluf, Yael Vinker, Lior Wolf, and Daniel Cohen-Or. Attend-and-excite:  
519 Attention-based semantic guidance for text-to-image diffusion models. *ACM transactions on*  
520 *Graphics (TOG)*, 42(4):1–10, 2023.

521 Haoran Chen, Junyan Lin, Xinhao Chen, Yue Fan, Xin Jin, Hui Su, Jianfeng Dong, Jinlan  
522 Fu, and Xiaoyu Shen. Rethinking visual layer selection in multimodal llms. *arXiv preprint*  
523 *arXiv:2504.21447*, 2025.

524 Lin Chen, Jinsong Li, Xiaoyi Dong, Pan Zhang, Yuhang Zang, Zehui Chen, Haodong Duan, Jiaqi  
525 Wang, Yu Qiao, Dahua Lin, et al. Are we on the right way for evaluating large vision-language  
526 models? *Advances in Neural Information Processing Systems*, 37:27056–27087, 2024a.

527 Meiqi Chen, Yixin Cao, Yan Zhang, and Chaochao Lu. Quantifying and mitigating unimodal biases  
528 in multimodal large language models: A causal perspective. In *Findings of the Association for*  
529 *Computational Linguistics: EMNLP 2024*, pp. 16449–16469, 2024b.

530 Zhe Chen, Jiannan Wu, Wenhui Wang, Weijie Su, Guo Chen, Sen Xing, Muyan Zhong, Qinglong  
531 Zhang, Xizhou Zhu, Lewei Lu, et al. Internvl: Scaling up vision foundation models and aligning  
532 for generic visual-linguistic tasks. In *Proceedings of the IEEE/CVF Conference on Computer*  
533 *Vision and Pattern Recognition*, pp. 24185–24198, 2024c.

540 Jacob Devlin, Ming-Wei Chang, Kenton Lee, and Kristina Toutanova. Bert: Pre-training of deep  
 541 bidirectional transformers for language understanding. In *Proceedings of the 2019 conference of*  
 542 *the North American chapter of the association for computational linguistics: human language*  
 543 *technologies, volume 1 (long and short papers)*, pp. 4171–4186, 2019.

544 Abhimanyu Dubey, Abhinav Jauhri, Abhinav Pandey, Abhishek Kadian, Ahmad Al-Dahle, Aiesha  
 545 Letman, Akhil Mathur, Alan Schelten, Amy Yang, Angela Fan, et al. The llama 3 herd of models.  
 546 *arXiv e-prints*, pp. arXiv–2407, 2024.

548 Rohit Girdhar, Alaaeldin El-Nouby, Zhuang Liu, Mannat Singh, Kalyan Vasudev Alwala, Armand  
 549 Joulin, and Ishan Misra. Imagebind: One embedding space to bind them all. In *Proceedings of*  
 550 *the IEEE/CVF Conference on Computer Vision and Pattern Recognition*, pp. 15180–15190, 2023.

551 Kristen Grauman, Andrew Westbury, Eugene Byrne, Zachary Chavis, Antonino Furnari, Rohit Gird-  
 552 har, Jackson Hamburger, Hao Jiang, Miao Liu, Xingyu Liu, et al. Ego4d: Around the world in  
 553 3,000 hours of egocentric video. In *Proceedings of the IEEE/CVF Conference on Computer Vision*  
 554 *and Pattern Recognition*, pp. 18995–19012, 2022.

555 Amir Hertz, Ron Mokady, Jay Tenenbaum, Kfir Aberman, Yael Pritch, and Daniel Cohen-or.  
 556 Prompt-to-prompt image editing with cross-attention control. In *The Eleventh International Con-  
 557 ference on Learning Representations*, 2023.

559 Edward J Hu, Phillip Wallis, Zeyuan Allen-Zhu, Yuanzhi Li, Shean Wang, Lu Wang, Weizhu Chen,  
 560 et al. Lora: Low-rank adaptation of large language models. In *International Conference on*  
 561 *Learning Representations*, 2022.

562 Lee Hyun, Kim Sung-Bin, Seungju Han, Youngjae Yu, and Tae-Hyun Oh. Smile: Multimodal  
 563 dataset for understanding laughter in video with language models. In *Findings of the Association*  
 564 *for Computational Linguistics: NAACL 2024*, pp. 1149–1167, 2024.

566 Wenqi Jia, Miao Liu, Hao Jiang, Ishwarya Ananthabhotla, James M Rehg, Vamsi Krishna Ithapu,  
 567 and Ruohan Gao. The audio-visual conversational graph: From an egocentric-exocentric perspec-  
 568 tive. In *Proceedings of the IEEE/CVF Conference on Computer Vision and Pattern Recognition*,  
 569 pp. 26396–26405, 2024.

570 Dohwan Ko, Sihyeon Kim, Yumin Suh, Minseo Yoon, Manmohan Chandraker, Hyunwoo J Kim,  
 571 et al. St-vlm: Kinematic instruction tuning for spatio-temporal reasoning in vision-language  
 572 models. *arXiv preprint arXiv:2503.19355*, 2025.

574 Fanqi Kong, Weiqin Zu, Xinyu Chen, Yaodong Yang, Song-Chun Zhu, and Xue Feng. Siv-  
 575 bench: A video benchmark for social interaction understanding and reasoning. *arXiv preprint*  
 576 *arXiv:2506.05425*, 2025.

577 Wessel Kraaij, Thomas Hain, Mike Lincoln, and Wilfried Post. The ami meeting corpus. In *Proc.*  
 578 *International Conference on Methods and Techniques in Behavioral Research*, pp. 1–4, 2005.

580 Bolin Lai, Hongxin Zhang, Miao Liu, Aryan Pariani, Fiona Ryan, Wenqi Jia, Shirley Anugrah  
 581 Hayati, James Rehg, and Diyi Yang. Werewolf among us: Multimodal resources for modeling  
 582 persuasion behaviors in social deduction games. In *Findings of the Association for Computational*  
 583 *Linguistics: ACL 2023*, pp. 6570–6588, 2023.

584 Sangmin Lee, Bolin Lai, Fiona Ryan, Bikram Boote, and James M Rehg. Modeling multimodal  
 585 social interactions: new challenges and baselines with densely aligned representations. In *Pro-  
 586 ceedings of the IEEE/CVF Conference on Computer Vision and Pattern Recognition*, pp. 14585–  
 587 14595, 2024a.

588 Sangmin Lee, Minzhi Li, Bolin Lai, Wenqi Jia, Fiona Ryan, Xu Cao, Ozgur Kara, Bikram Boote,  
 589 Weiyan Shi, Diyi Yang, et al. Towards social ai: A survey on understanding social interactions.  
 590 *arXiv preprint arXiv:2409.15316*, 2024b.

592 Jie Lei, Licheng Yu, Mohit Bansal, and Tamara Berg. Tqva: Localized, compositional video ques-  
 593 tion answering. In *Proceedings of the 2018 Conference on Empirical Methods in Natural Lan-  
 guage Processing*, pp. 1369–1379, 2018.

594 Jie Lei, Licheng Yu, Tamara Berg, and Mohit Bansal. Tqvqa+: Spatio-temporal grounding for video  
 595 question answering. In *Proceedings of the 58th Annual Meeting of the Association for Computa-*  
 596 *tional Linguistics*, pp. 8211–8225, 2020.

597

598 Xinpeng Li, Shijian Deng, Bolin Lai, Weiguo Pian, James M Rehg, and Yapeng Tian. Towards  
 599 online multi-modal social interaction understanding. *arXiv preprint arXiv:2503.19851*, 2025a.

600 Zongxia Li, Xiyang Wu, Hongyang Du, Fuxiao Liu, Huy Nghiem, and Guangyao Shi. A survey of  
 601 state of the art large vision language models: Alignment, benchmark, evaluations and challenges.  
 602 *arXiv preprint arXiv:2501.02189*, 2025b.

603

604 Lili Liang, Guanglu Sun, Tianlin Li, Shuai Liu, and Weiping Ding. Tlnet: Temporal span localiza-  
 605 tion network with collaborative graph reasoning for video question answering. *IEEE Transactions*  
 606 *on Emerging Topics in Computational Intelligence*, 2024a.

607 Yaoyuan Liang, Zhuojun Cai, Jian Xu, Guanbo Huang, Yiran Wang, Xiao Liang, Jiahao Liu, Ziran  
 608 Li, Jingang Wang, and Shao-Lun Huang. Unleashing region understanding in intermediate lay-  
 609 ers for mllm-based referring expression generation. *Advances in Neural Information Processing*  
 610 *Systems*, 37:120578–120601, 2024b.

611

612 Tsung-Yi Lin, Michael Maire, Serge Belongie, James Hays, Pietro Perona, Deva Ramanan, Piotr  
 613 Dollár, and C Lawrence Zitnick. Microsoft coco: Common objects in context. In *European*  
 614 *conference on computer vision*, pp. 740–755. Springer, 2014.

615

616 Haotian Liu, Chunyuan Li, Qingyang Wu, and Yong Jae Lee. Visual instruction tuning. *Advances*  
 617 *in neural information processing systems*, 36:34892–34916, 2023.

618

619 Leena Mathur, Paul Pu Liang, and Louis-Philippe Morency. Advancing social intelligence in ai  
 620 agents: Technical challenges and open questions. In *Proceedings of the 2024 Conference on*  
 621 *Empirical Methods in Natural Language Processing*, pp. 20541–20560, 2024.

622

623 Leena Mathur, Marian Qian, Paul Pu Liang, and Louis-Philippe Morency. Social genome: Grounded  
 624 social reasoning abilities of multimodal models. *arXiv preprint arXiv:2502.15109*, 2025.

625

626 Xinyi Mou, Xuanwen Ding, Qi He, Liang Wang, Jingcong Liang, Xinnong Zhang, Libo Sun, Jiayu  
 627 Lin, Jie Zhou, Xuanjing Huang, et al. From individual to society: A survey on social simulation  
 628 driven by large language model-based agents. *arXiv preprint arXiv:2412.03563*, 2024.

629

630 Philipp Müller, Michael Xuelin Huang, and Andreas Bulling. Detecting low rapport during natural  
 631 interactions in small groups from non-verbal behaviour. In *Proceedings of the 23rd International*  
 632 *Conference on Intelligent User Interfaces*, pp. 153–164, 2018.

633

634 Philipp Müller, Michael Dietz, Dominik Schiller, Dominike Thomas, Guanhua Zhang, Patrick Geb-  
 635 hard, Elisabeth André, and Andreas Bulling. Multimediate: Multi-modal group behaviour analy-  
 636 sis for artificial mediation. In *Proceedings of the 29th ACM International Conference on Multi-*  
 637 *media*, pp. 4878–4882, 2021.

638

639 Curtis G Northcutt, Shengxin Zha, Steven Lovegrove, and Richard Newcombe. Egocom: A multi-  
 640 person multi-modal egocentric communications dataset. *IEEE Transactions on Pattern Analysis*  
 641 *and Machine Intelligence*, 45(6):6783–6793, 2020.

642

643 Eunkyu Park, Wesley Hanwen Deng, Gunhee Kim, Motahhare Eslami, and Maarten Sap. Cogni-  
 644 tive chain-of-thought: Structured multimodal reasoning about social situations. *arXiv preprint*  
 645 *arXiv:2507.20409*, 2025a.

646

647 Jean Park, Kuk Jin Jang, Basam Alasaly, Sriharsha Mopidevi, Andrew Zolensky, Eric Eaton, In-  
 648 sup Lee, and Kevin Johnson. Assessing modality bias in video question answering benchmarks  
 649 with multimodal large language models. In *Proceedings of the AAAI Conference on Artificial*  
 650 *Intelligence*, volume 39, pp. 19821–19829, 2025b.

651

652 Adam Paszke, Sam Gross, Francisco Massa, Adam Lerer, James Bradbury, Gregory Chanan, Trevor  
 653 Killeen, Zeming Lin, Natalia Gimelshein, Luca Antiga, et al. Pytorch: An imperative style, high-  
 654 performance deep learning library. *Advances in neural information processing systems*, 32, 2019.

648 Renjie Pi, Tianyang Han, Wei Xiong, Jipeng Zhang, Runtao Liu, Rui Pan, and Tong Zhang.  
 649 Strengthening multimodal large language model with bootstrapped preference optimization. In  
 650 *European Conference on Computer Vision*, pp. 382–398. Springer, 2024.

651

652 Alec Radford, Jeffrey Wu, Rewon Child, David Luan, Dario Amodei, Ilya Sutskever, et al. Language  
 653 models are unsupervised multitask learners. *OpenAI blog*, 1(8):9, 2019.

654 Alec Radford, Jong Wook Kim, Chris Hallacy, Aditya Ramesh, Gabriel Goh, Sandhini Agarwal,  
 655 Girish Sastry, Amanda Askell, Pamela Mishkin, Jack Clark, et al. Learning transferable visual  
 656 models from natural language supervision. In *International conference on machine learning*, pp.  
 657 8748–8763. PMLR, 2021.

658

659 Fiona Ryan, Hao Jiang, Abhinav Shukla, James M Rehg, and Vamsi Krishna Ithapu. Egocentric  
 660 auditory attention localization in conversations. In *Proceedings of the IEEE/CVF Conference on*  
 661 *Computer Vision and Pattern Recognition*, pp. 14663–14674, 2023.

662 Aleksandar Shtedritski, Christian Rupprecht, and Andrea Vedaldi. What does clip know about a  
 663 red circle? visual prompt engineering for vlms. In *Proceedings of the IEEE/CVF International*  
 664 *Conference on Computer Vision*, pp. 11987–11997, 2023.

665

666 Wenxuan Song, Ziyang Zhou, Han Zhao, Jiayi Chen, Pengxiang Ding, Haodong Yan, Yuxin Huang,  
 667 Feilong Tang, Donglin Wang, and Haoang Li. Reconvla: Reconstructive vision-language-action  
 668 model as effective robot perceiver. *arXiv preprint arXiv:2508.10333*, 2025.

669

670 Zhiqing Sun, Sheng Shen, Shengcao Cao, Haotian Liu, Chunyuan Li, Yikang Shen, Chuang Gan,  
 671 Liangyan Gui, Yu-Xiong Wang, Yiming Yang, et al. Aligning large multimodal models with  
 672 factually augmented rlhf. In *Findings of the Association for Computational Linguistics ACL*  
 2024, pp. 13088–13110, 2024.

673

674 Feilong Tang, Chengzhi Liu, Zhongxing Xu, Ming Hu, Zile Huang, Haochen Xue, Ziyang Chen,  
 675 Zelin Peng, Zhiwei Yang, Sijin Zhou, et al. Seeing far and clearly: Mitigating hallucinations in  
 676 mllms with attention causal decoding. In *Proceedings of the IEEE/CVF Conference on Computer*  
 677 *Vision and Pattern Recognition*, pp. 26147–26159, 2025.

678

679 Shengbang Tong, Zhuang Liu, Yuexiang Zhai, Yi Ma, Yann LeCun, and Saining Xie. Eyes wide  
 680 shut? exploring the visual shortcomings of multimodal llms. In *Proceedings of the IEEE/CVF*  
 681 *Conference on Computer Vision and Pattern Recognition*, pp. 9568–9578, 2024.

682

683 Ashish Vaswani, Noam Shazeer, Niki Parmar, Jakob Uszkoreit, Llion Jones, Aidan N Gomez,  
 684 Łukasz Kaiser, and Illia Polosukhin. Attention is all you need. *Advances in neural information*  
 685 *processing systems*, 30, 2017.

686

687 Elena Voita, David Talbot, Fedor Moiseev, Rico Sennrich, and Ivan Titov. Analyzing multi-head  
 688 self-attention: Specialized heads do the heavy lifting, the rest can be pruned. In *Proceedings of*  
 689 *the 57th Annual Meeting of the Association for Computational Linguistics*, pp. 5797–5808, 2019.

690

691 Wei-Yao Wang, Zhao Wang, Helen Suzuki, and Yoshiyuki Kobayashi. Seeing is understanding:  
 692 Unlocking causal attention into modality-mutual attention for multimodal llms. *arXiv preprint*  
 693 *arXiv:2503.02597*, 2025.

694

695 Mingrui Wu, Xinyue Cai, Jiayi Ji, Jiale Li, Oucheng Huang, Gen Luo, Hao Fei, Guannan Jiang, Xi-  
 696 aoshuai Sun, and Rongrong Ji. Controlmllm: Training-free visual prompt learning for multimodal  
 697 large language models. *Advances in Neural Information Processing Systems*, 37:45206–45234,  
 698 2024a.

699

700 Tao Wu, Mengze Li, Jingyuan Chen, Wei Ji, Wang Lin, Jinyang Gao, Kun Kuang, Zhou Zhao, and  
 701 Fei Wu. Semantic alignment for multimodal large language models. In *Proceedings of the 32nd*  
 702 *ACM International Conference on Multimedia*, pp. 3489–3498, 2024b.

703

704 Yuhang Wu, Wenmeng Yu, Yean Cheng, Yan Wang, Xiaohan Zhang, Jiazheng Xu, Ming Ding, and  
 705 Yuxiao Dong. Alignmmbench: Evaluating chinese multimodal alignment in large vision-language  
 706 models. *arXiv preprint arXiv:2406.09295*, 2024c.

702 Junbin Xiao, Angela Yao, Yicong Li, and Tat-Seng Chua. Can i trust your answer? visually grounded  
 703 video question answering. In *Proceedings of the IEEE/CVF Conference on Computer Vision and*  
 704 *Pattern Recognition*, pp. 13204–13214, 2024.

705 Yun Xing, Yiheng Li, Ivan Laptev, and Shijian Lu. Mitigating object hallucination via concentric  
 706 causal attention. *Advances in neural information processing systems*, 37:92012–92035, 2024.

708 Kun Yan, Zeyu Wang, Lei Ji, Yuntao Wang, Nan Duan, and Shuai Ma. Voila-a: Aligning vision-  
 709 language models with user’s gaze attention. *Advances in Neural Information Processing Systems*,  
 710 37:1890–1918, 2024.

711 Xiang Yue, Tianyu Zheng, Yuansheng Ni, Yubo Wang, Kai Zhang, Shengbang Tong, Yuxuan Sun,  
 712 Botao Yu, Ge Zhang, Huan Sun, et al. Mmmu-pro: A more robust multi-discipline multimodal  
 713 understanding benchmark. *arXiv preprint arXiv:2409.02813*, 2024.

715 Amir Zadeh, Michael Chan, Paul Pu Liang, Edmund Tong, and Louis-Philippe Morency. Social-  
 716 iq: A question answering benchmark for artificial social intelligence. In *Proceedings of the*  
 717 *IEEE/CVF Conference on Computer Vision and Pattern Recognition*, pp. 8807–8817, 2019.

718 Jiarui Zhang, Mahyar Khayatkhoei, Prateek Chhikara, and Filip Ilievski. Mllms know where to  
 719 look: Training-free perception of small visual details with multimodal llms. In *The Thirteenth*  
 720 *International Conference on Learning Representations*, 2025a.

722 Yi-Fan Zhang, Weichen Yu, Qingsong Wen, Xue Wang, Zhang Zhang, Liang Wang, Rong Jin, and  
 723 Tieniu Tan. Debiasing multimodal large language models. *arXiv preprint arXiv:2403.05262*,  
 724 2024.

725 YiFan Zhang, Tao Yu, Haochen Tian, Chaoyou Fu, Peiyan Li, Jianshu Zeng, Wulin Xie, Yang Shi,  
 726 Huanyu Zhang, Junkang Wu, et al. Mm-rlhf: The next step forward in multimodal llm alignment.  
 727 In *Forty-second International Conference on Machine Learning*, 2025b.

729 Zefeng Zhang, Hengzhu Tang, Jiawei Sheng, Zhenyu Zhang, Yiming Ren, Zhenyang Li, Dawei Yin,  
 730 Duohe Ma, and Tingwen Liu. Debiasing multimodal large language models via noise-aware pref-  
 731 erence optimization. In *Proceedings of the IEEE/CVF Conference Computer Vision and Pattern*  
 732 *Recognition*, pp. 9423–9433, 2025c.

733 Zhenxing Zhang, Yaxiong Wang, Lechao Cheng, Zhun Zhong, Dan Guo, and Meng Wang. Asap:  
 734 Advancing semantic alignment promotes multi-modal manipulation detecting and grounding. In  
 735 *Proceedings of the IEEE/CVF Conference on Computer Vision and Pattern Recognition*, pp.  
 736 4005–4014, 2025d.

737 Xu Zheng, Chenfei Liao, Yuqian Fu, Kaiyu Lei, Yuanhuiyi Lyu, Lutao Jiang, Bin Ren, Jialei Chen,  
 738 Jiawen Wang, Chengxin Li, et al. Mllms are deeply affected by modality bias. *arXiv preprint*  
 739 *arXiv:2505.18657*, 2025.

741 Yaowei Zheng, Richong Zhang, Junhao Zhang, YeYanhan YeYanhan, and Zheyuan Luo. Llamafac-  
 742 tory: Unified efficient fine-tuning of 100+ language models. In *Proceedings of the 62nd Annual*  
 743 *Meeting of the Association for Computational Linguistics (Volume 3: System Demonstrations)*,  
 744 pp. 400–410, 2024.

745 Qi Zhou, Wannapon Suraworachet, and Mutlu Cukurova. Detecting non-verbal speech and gaze  
 746 behaviours with multimodal data and computer vision to interpret effective collaborative learning  
 747 interactions. *Education and information technologies*, 29(1):1071–1098, 2024.

748  
 749  
 750  
 751  
 752  
 753  
 754  
 755

756 **A APPENDIX**  
757758 **A.1 TASKS INSTRUCTIONS**  
759760 We evaluate our method on four types of social interaction tasks. Each task takes as input the  
761 video frames, transcripts, and speaker bounding boxes. We describe the tasks and prompts used for  
762 MLLMs below:763 

- 764 **Video Question Answering.** This task requires answering questions grounded in multi-party  
765 dialogue videos. In TVQA+ (Lei et al., 2020), each question is accompanied by five candidate  
766 choices. Instruction prompt: <video>\nWatch this video of speakers social  
767 interaction, read their conversation, question and choose the  
768 correct answer. {Conversation}. Q: How does Sheldon feel? a0:  
769 tired, ..., a4: angry.
- 770 **Speaking Target Identification.** This task identifies the addressee (speaking target) of  
771 the current speaker in the dialogue. Instruction prompt: <video>\nWatch this  
772 video of {N} speakers social interaction, be aware of their  
773 non-verbal behaviours. Read the conversation. {Conversation}.  
774 Predict the speaking target (speaking to whom) of this sentence:  
775 Speaker 0: Who were you?
- 776 **Pronoun Coreference Resolution.** This task aims to resolve pronouns in the dialogue transcripts  
777 to their corresponding speakers. Instruction prompt: <video>\nWatch this video  
778 of {N} speakers social interaction, be aware of their non-verbal  
779 behaviours. Read the conversation. {Conversation}. Predict  
780 which speaker should be the 'he' in this sentence: Speaker 1:  
781 Did he not say that?
- 782 **Mentioned Player Prediction.** This task requires linking a dialogue mentioned name to  
783 the correct participant appearing in the video. Instruction prompt: <video>\nWatch  
784 this video of {N} speakers social interaction, be aware of their  
785 non-verbal behaviours. Read the conversation. {Conversation}.  
786 Predict which speaker should be the 'Mitchell' in this sentence:  
787 Speaker 3: I think it's Mitchell.

788 **A.2 BASELINE METHODS**

789 We compare our method against several baseline approaches in table 2, described as follows:

790 

- 791 **Random.** For the VQA task, the model randomly selects one answer from five candidates. For  
792 MMSI tasks, it randomly selects one speaker among  $N$  candidates.
- 793 **ST-VLM-7B (Ko et al., 2025) and TLNet (Liang et al., 2024a)** are highly competitive models on  
794 TVQA+. However, since our setting requires at least one speaker with bounding box annotations,  
795 our training and test sets differ from theirs. Despite this difference, our method substantially  
796 outperforms these baselines.
- 797 **MMSI (Lee et al., 2024a)** employs a transformer to align and fuse text features from language  
798 models with visual interaction features derived from bounding boxes and keypoints. Classification  
799 tasks are then performed via a masked modeling objective to solve three social interaction tasks.  
800 We report their best-performing result, i.e., the RoBERTa-based baseline, for comparison.
- 801 **OnlineMMSI (Li et al., 2025a)** leverages bounding boxes and keypoints as visual prompts to  
802 align multiple speakers for MLLMs. Since the implementation was not publicly released, we  
803 re-implemented it based on Qwen2.5-VL, using only bounding box annotations for a fair compar-  
804 ison. Notably, our reproduced results are even higher than original reported numbers, which may  
805 be due to preprocessing differences, but this does not affect the fairness of comparison.
- 806 **Qwen2.5-Text (Bai et al., 2025)** is a text-only baseline where Qwen2.5-VL is given only the  
807 dialogue transcripts without any video input.
- 808 **Qwen2.5-VL (Bai et al., 2025)** is a strong MLLM baseline. We use the instruction prompt  
809 described in appendix A.1, but additionally append bounding box coordinates as text prompts,  
e.g., Speaker 1 [100, 100, 300, 400].